Current Biology 23, 1215–1220, July 8, 2013 ©2013 Elsevier Ltd All rights reserved http://dx.doi.org/10.1016/j.cub.2013.05.027

Report

# Polarity in Migrating Neurons Is Related to a Mechanism Analogous to Cytokinesis

**Aditi Falnikar,[1] Shubha Tole,[2] Mei Liu,[3] Judy S. Liu,[4] and Peter W. Baas[1,*]**

[1]Department of Neurobiology and Anatomy, Drexel University College of Medicine, 2900 Queen Lane, Philadelphia, PA 19129, USA

[2]Department of Biological Sciences, Tata Institute of Fundamental Research, Colaba, Mumbai 400 005, India

[3]Jiangsu Key Laboratory of Neuroregeneration, Nantong University, Nantong 226001, China

[4]Center for Neuroscience Research, Children's National Medical Center, 111 Michigan Avenue NW, Washington, DC 20010, USA

## Summary

**Migrating neurons are bipolar, with a leading process and a trailing process [1]. The proximal region of the leading process displays a concentration of F-actin that contributes to the advance of the soma and the centrosome [2–7]. Here, we show that kinesin-6, a microtubule-based motor protein best known for its role in cytokinesis, also concentrates in this region. Depletion of kinesin-6 results in multipolar neurons that either are stationary or continuously change their direction of movement. In such neurons, F-actin no longer concentrates in a single process. During cytokinesis, kinesin-6 forms a complex with a Rho-family GTPase-activating protein called MgcRacGAP to signal to the actin cytoskeleton so that cortical movements are concentrated in the cleavage furrow [8–13]. During neuronal migration, MgcRacGap also concentrates in the proximal region of the leading process, and inhibition of its activity results in a phenotype similar to kinesin-6 depletion. We conclude that neuronal migration utilizes a cytoskeletal pathway analogous to cytokinesis, with kinesin-6 signaling through MgcRacGap to the actin cytoskeleton to constrain process number and restrict protrusive activity to a single leading process, thus resulting in a bipolar neuron able to move in a directed fashion.**

## Results and Discussion

### Kinesin-6 Depletion Results in Altered Migration and Morphology of Cortical Neurons In Vivo

Three EGFP-containing plasmids, kinesin-6 small hairpin RNA (shRNA) coding, corresponding scrambled control, or empty vector, were individually electroporated into cortical ventricular zones of embryonic day 14 (E14) mice (for details and of this and other procedures, see the Supplemental Experimental Procedures available online; efficiency of knockdown is shown in Figure 1E). Similar numbers of fluorescent cells appeared in all groups, but with slightly fewer in the kinesin-6 shRNA group, consistent with cytokinesis failure leading to cell death of neural progenitors [14, 15]. No differences in radial glial cells were observed among the groups (data not shown), indicating that observed effects on neuronal migration were not due to alterations in the scaffold along which migration occurs.

Each section was divided into three bins: upper, middle, and lower. As expected [16, 17], most cells reached the upper bin in the case of the empty vector and scrambled control groups (Figures 1A and 1F; 74.5% ± 4.5% and 63.2% ± 5.1%, respectively; no significant difference). In the kinesin-6 shRNA group, most cells were stalled in the lower bin (Figures 1B and 1F); only 7.3% ± 2.2% cells were found in the upper bin (significant difference with the empty vector and scrambled control in both the upper bin [$p < 0.0001$ and $p < 0.0001$, respectively] and the lower bin [$p < 0.0001$ and $p < 0.0001$, respectively, Student's t test]).

As they enter the cortical intermediate zone region from the subventricular zone region, neurons normally transform from a multipolar to a bipolar morphology suitable for directed migration [18, 19]. In the kinesin-6 shRNA group, most cells in this region were multipolar (Figures 1D and 1G; 91.1% ± 6%), unlike the empty vector and the scrambled control groups (Figures 1C and 1G; 32.8% ± 4.4% and 36.6% ± 3% were multipolar, respectively) (no significant difference between the empty vector and scrambled control groups; kinesin-6 shRNA group was significantly different from each of the other two groups [$p = 0.008$ and $p = 0.007$ respectively, Student's t test]). Many cells were bipolar in the empty vector and the scrambled control groups (60.4% ± 5.5% and 49.3% ± 3.1%, respectively), but very few were bipolar in this region in the kinesin-6 shRNA group (4.2% ± 3%).

### Kinesin-6 Depletion Alters Cortical Neuron Migration along Fiber Lattice In Vitro

In a culture system of cortical neurons migrating along glial fibers in vitro [20], neurons transfected with kinesin-6 shRNA assumed a multipolar morphology and were more or less immobile (Figures S1C and S1D), whereas cells transfected with scrambled control migrated rapidly (Figures S1A and S1B). Mean migration speed of control neurons was 40.4 ± 4.8 μm/hr ($n = 14$), while that of kinesin-6 shRNA neurons was 15.6 ± 3.7 μm/hr ($n = 11$) (significant difference [$p = 0.0007$, Student's t test]).

### Kinesin-6 Depletion Affects Migration of Cerebellar Granule Neurons In Vitro

For mechanistic studies, cerebellar granule neurons were transfected with small interfering RNA (siRNA) (control or kinesin-6) and pEGFP-C1 and then plated on glass. Efficiency of knockdown is shown in Figure 2A. Time-lapse imaging indicated that while control neurons moved in a unidirectional fashion (Figure 2B), kinesin-6-depleted neurons frequently changed direction of migration (Figure 2C; see also Movie S1). While control neurons exhibited an average net displacement of 26.3 ± 2.0 μm/hr ($n = 17$), kinesin-6-depleted neurons exhibited little average net displacement (6.7 ± 1.0 μm/hr, $n = 14$, $p < 0.0001$, Student's t test; Figure 2D). Thus, kinesin-6 depletion did not render these neurons stationary as with the cortical neurons but perturbed directed movement, as reflected by a decrease in the persistence of movement (Figures 2E and 2F).

*Correspondence: pbaas@drexelmed.edu

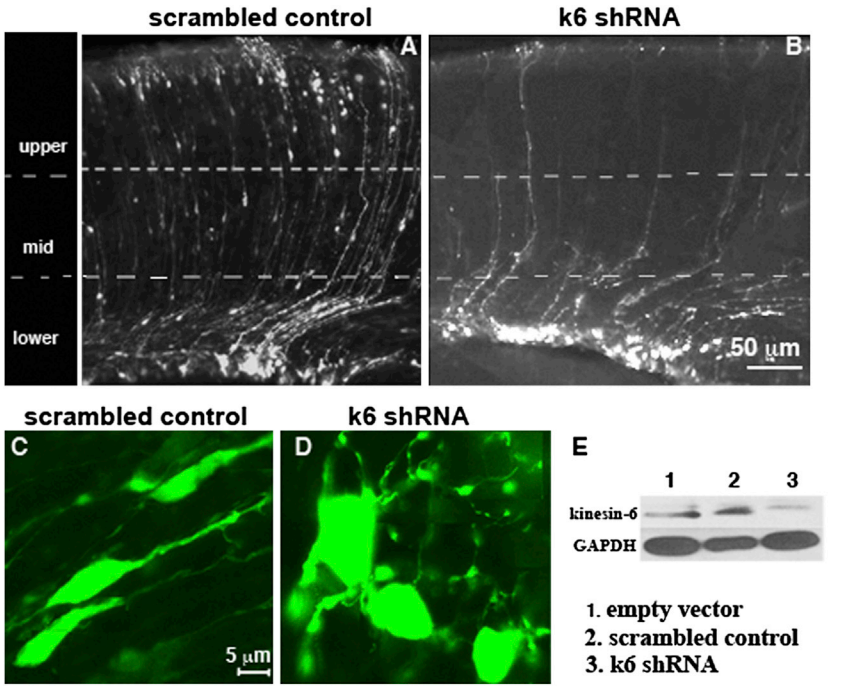


Figure 1. Altered Distribution and Morphology of Cortical Neurons after In Utero Electroporation of Kinesin-6 shRNA

(A, B, and F) Coronal sections from brains electroporated with scrambled control shRNA (A) or kinesin-6 shRNA (B) at embryonic day 14 (E14) and harvested at postnatal day 1 (P1). Quantification of cell distribution in the three bins is shown in (F). For the empty vector group, n = 4 brains and 1,152 cells from six sections were counted. For the scrambled control group, n = 3 brains and 739 cells from five sections were counted. For the kinesin-6 shRNA group, n = 4 brains and 524 cells from ten sections were counted.

(C, D, and G) Morphology of cells in the subventricular zone in coronal sections generated after in utero electroporation of scrambled control shRNA (C) and kinesin-6 shRNA (D), respectively. Quantification of cell morphology is shown in (G). Error bars represent SEM.

(E) Western blot for kinesin-6 and glyceraldehyde-3-phosphate (GAPDH) (loading control) in NIH 3T3 cells transfected with control empty vector, scrambled control shRNA, or kinesin-6 shRNA after 72 hr, showing approximately 70% depletion of kinesin-6 protein. Migration of cortical neurons was also analyzed in vitro (see Figure S1).

While most control neurons exhibited a bipolar morphology with a prominent leading process and a thin trailing process, kinesin-6-depleted neurons were usually multipolar (Figures 2H and 2J). Most often these cells had three processes, two of which were morphologically similar and a third that was thinner and more similar to the trailing process of control neurons (see Figure 3D for morphological analyses on fixed cells). Morphological analyses on live cells indicated that the proportion of multipolar cells was significantly higher at 92.9% (n = 14) in the kinesin-6 siRNA group compared to the control group, in which the proportion was 7.1% (n = 17) (Figure 2J; $p < 0.0001$, chi-square test). This phenotype was rescued by expression of siRNA-resistant kinesin-6-GFP (Figure 2J; n = 25). When the angle between the two similar processes (plotted against the speed of migration on a per cell basis; see Figure 2I) was closer to 180° (or 0°), migration speeds were higher. When the angle was 60°–120°, the speeds were lower, suggesting that altered morphology is at least partially responsible for altered migration. Overexpression of kinesin-6 caused slight bundling of microtubules and reduced the length of the leading process by 36.3% (Figures S2, S2F, and S2F′; n = 8 in each group, $p < 0.0001$).

Movement of the centrosome, observed with red fluorescent protein (RFP)-tagged pericentrin, consistently preceded that of the caudal tip in the control siRNA group (Figures S2A and S2A′). By contrast, in the kinesin-6-depleted group, the caudal tip and the centrosome sometimes overlapped (Figures S2B and S2B′). In the control siRNA group, for 88.9% of the cells, the centrosome was consistently situated in the anterior soma, but that was true for only 10% of the cells in the kinesin-6 siRNA group (n = 27 for the control siRNA group and n = 20 for the kinesin-6 siRNA group, $p < 0.0001$, Fisher's exact test; see Figure S2C).

## Kinesin-6 Is Enriched in the Proximal Region of the Leading Process

The immunostain signal for kinesin-6 was more intense in the proximal region of the leading process compared to its distal region (Figures 3A–3A‴). The regions rich in kinesin-6 were typically less concentrated with microtubules than other regions of the leading process, indicating a true enrichment of kinesin-6 relative to microtubule mass (Figure 3B). This was further confirmed by comparison to EGFP as a volume marker (data not shown). In most of these neurons, the centrosome was situated within this enriched region (92.9%; see Figures S2D–S2D″ and S2E–S2E″ for micrographs). Correlation between kinesin-6 enrichment and centrosome localization was significant ($p = 0.001$ [Pearson's correlation coefficient] between the "centrosome only" group and "both" group and $p = 0.005$ between the "enrichment only" and "both" group, total n = 16). Interestingly, there was a strong correlation between kinesin-6 and F-actin enrichments ($p = 0.0008$ [Pearson's correlation coefficient] between the "actin only"

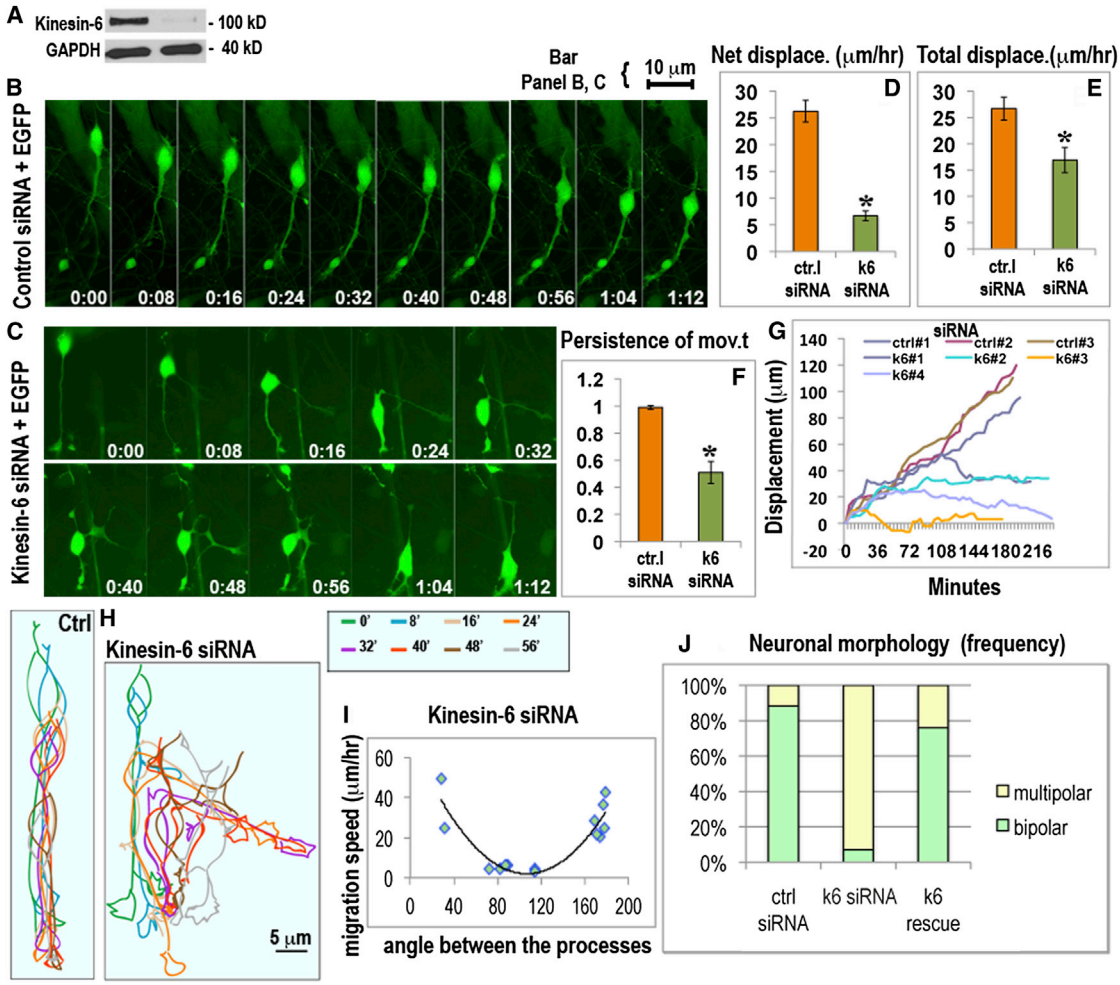


Figure 2. Effect of siRNA-Mediated Depletion of Kinesin-6 on Migration and Morphology of Cerebellar Granule Neurons In Vitro

(A) Western blot for kinesin-6 and GAPDH in dissociated cerebellar cells transfected with control siRNA (left lane) or kinesin-6 siRNA (right lane) for 72 hr, showing >90% depletion of kinesin-6 protein.

(B and C) Migration of cerebellar neurons cotransfected with control siRNA + EGFP (B) and kinesin-6 siRNA + EGFP (C) as represented by images captured 4 min apart. See also Movie S1.

(D–F) Average net displacement per hour (D), average total displacement per hour (E), and average persistence of movement (F) for control and kinesin-6-depleted neurons. Error bars represent SEM.

(G) Tracings of movements of somas of three control neurons (upper three lines) and four kinesin-6-depleted neurons (lower four lines).

(H) Tracings of cell shape of a migrating neuron transfected with control siRNA (left) or kinesin-6 siRNA (right). Different time frames were traced in different colors; color coding is shown in the box to the upper right.

(I) Correlation between angle between processes and migration speeds for individual cells for the kinesin-6 siRNA group.

(J) Quantification of cell morphology in control, kinesin-6 siRNA, and "kinesin-6 siRNA + kinesin-6-GFP" (k6 rescue) groups. See Figure S2 for the effect of kinesin-6 depletion on centrosome movements and the kinesin-6 overexpression phenotype.

and "both" groups and also between the "kinesin-6 only" and "both" groups), which might relate to the fact that kinesin-6 has an actin-binding domain [21].

### F-Actin Is Mislocalized in Kinesin-6-Depleted Granule Neurons

Phalloidin staining showed F-actin enriched in the proximal leading process (Figures 3C–3C‴) of control neurons. Because kinesin-6-depleted neurons were generally multipolar, no one process was clearly identifiable as the leader. Whereas in control cells the leading process was consistently and significantly thicker than the trailing process (mean thickness for the leading process, 1.2 ± 0.01 μm; mean thickness for the trailing process, 0.4 ± 0.01 μm; n = 36; Figure 3D), kinesin-6-depleted cells typically had three processes, two of which were of comparable thickness while the third process was usually thinner (mean thickness for processes, 0.7 ± 0.01 μm, 0.7 ± 0.01 μm, and 0.4 ± 0.01 μm; n = 34). In phalloidin-stained control cells, 54.9% cells did not show any F-actin enrichment, 35.3% cells showed enrichment in the leading process, and 9.8% cells showed enrichment in multiple processes (n = 51). This is consistent with previous studies indicating that proximal F-actin enrichment occurs only when the cell is making a forward step and hence would not be expected to be in every cell at all times [3]. In kinesin-6-depleted cultures, 52.6% of cells did not show any F-actin enrichment and 7.0% of cells showed enrichment in a single process, whereas 23% of cells showed enrichment in multiple

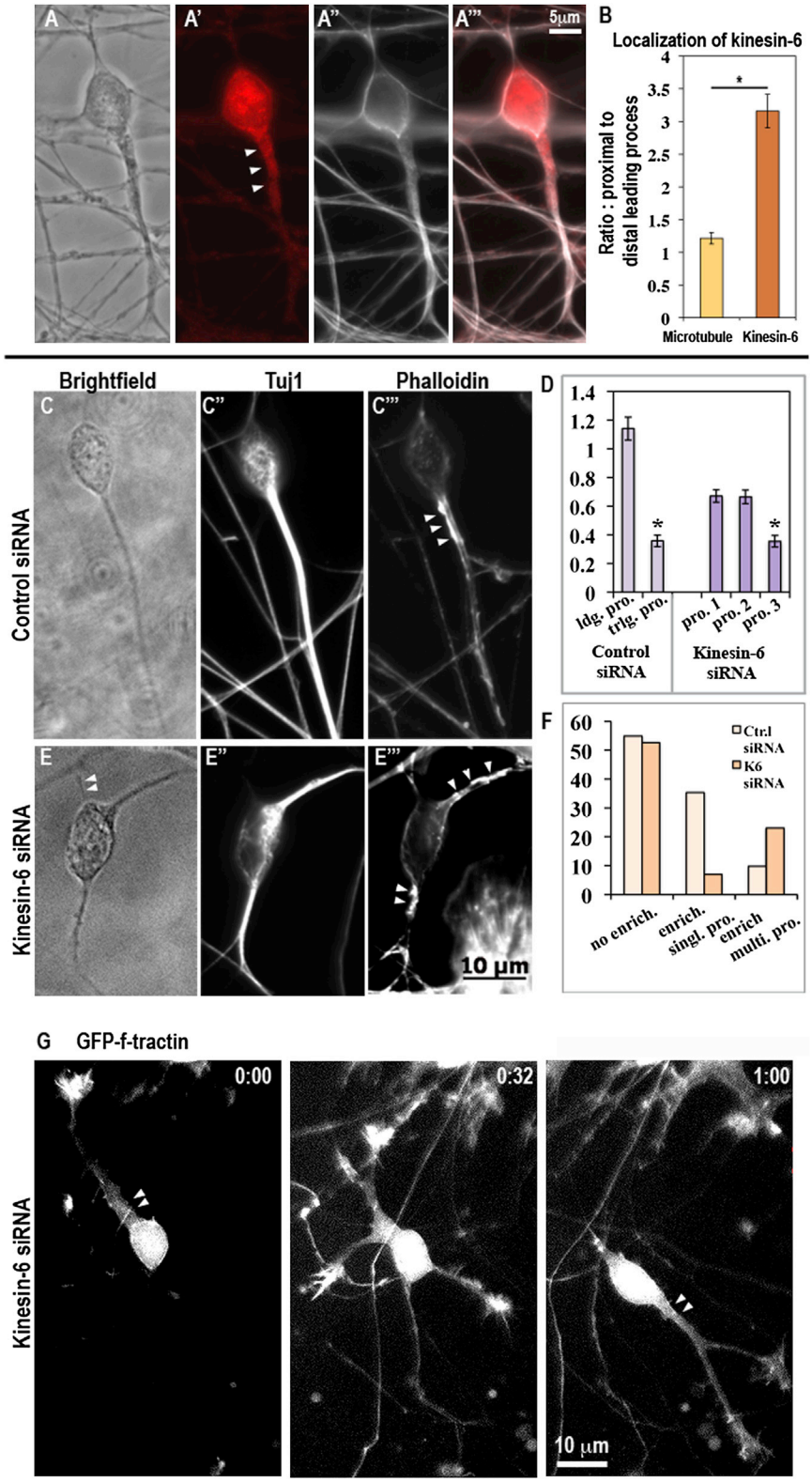


Figure 3. Kinesin-6 Immunostaining in Cultured Cerebellar Granule Neurons and Effect on Actin Distribution

(A–A‴ and B) Coimmunostaining for kinesin-6 and α-tubulin (to reveal microtubules) in a cerebellar granule neuron. Note that α-tubulin (microtubule) staining does not show enrichment in the proximal leading process, whereas kinesin-6 staining is enriched.

(C–C‴ and E–E‴) Immunostaining for Tuj1 (neuron-specific β-III-tubulin) and simultaneous staining with phalloidin to detect F-actin on neurons transfected with control siRNA (C–C‴) or kinesin-6 siRNA (E–E‴) after 72 hr. In the control siRNA group, a subset of cells showed strong F-actin enrichment in specific subcellular regions. In this subset, this enrichment was typically restricted to the proximal region of a single leading process, whereas in the kinesin-6 siRNA group, F-actin enrichment was often observed simultaneously in multiple processes. Arrowheads indicate F-actin-enriched regions.

(D) Quantification of cellular morphology in terms of process thickness for cells transfected with control or kinesin-6 siRNA. In the control group, neurons possessed a single leading process, which can be defined by greater thickness of this process, whereas in the kinesin-6 group, neurons typically possessed three processes, two of which were of similar thickness. Effect of kinesin-6 depletion on microtubule dynamics was also analyzed (see Figure S3).

(F) Quantification of the proportion of neurons showing F-actin enrichment in the total population, and pattern of actin enrichment within this subset, in cultures that were transfected with control siRNA or kinesin-6 siRNA for 72 hr.

(G) Live imaging of F-actin using GFP-F-tractin probe in kinesin-6-depleted cells.

processes (n = 57; see Figures 3C–3C‴, 3E–3E‴, and 3F). The difference between the control siRNA and kinesin-6 siRNA group, with regard to percentage of cells showing F-actin enrichment in a single process and that in multiple processes, was found to be significant via a 2 × 2 contingency table test ($p < 0.0001$). Rate of F-actin turnover in the proximal leading process is higher than within other cellular compartments [3]. No detectable differences in the dynamics of the actin enrichments in control and kinesin-6-depleted neurons were observed when F-actin dynamics were probed using time-lapse microscopy on GFP-F-tractin-transfected neurons (Figure 3G; see Supplemental Experimental Procedures).

### Changes in Microtubule Organization in Kinesin-6-Depleted Migratory Neurons

Neurons were cotransfected with kinesin-6 or control siRNA, RFP-Pct (to label the centrosome), and EGFP-EB3 (to label growing microtubule plus ends, which appear as fluorescent comets). Comets filled the leading process and curved around the nucleus in the soma (still images in Figures S3A and S3B). Comet speed was indistinguishable in controls (0.21 ± 0.02 μm/s) and kinesin-6-depleted cells (0.23 ± 0.01 μm/s). In the control leading process and soma, most comets emerged and projected away from the centrosome (93.8% ± 1% and 93.7% ± 3.3%,

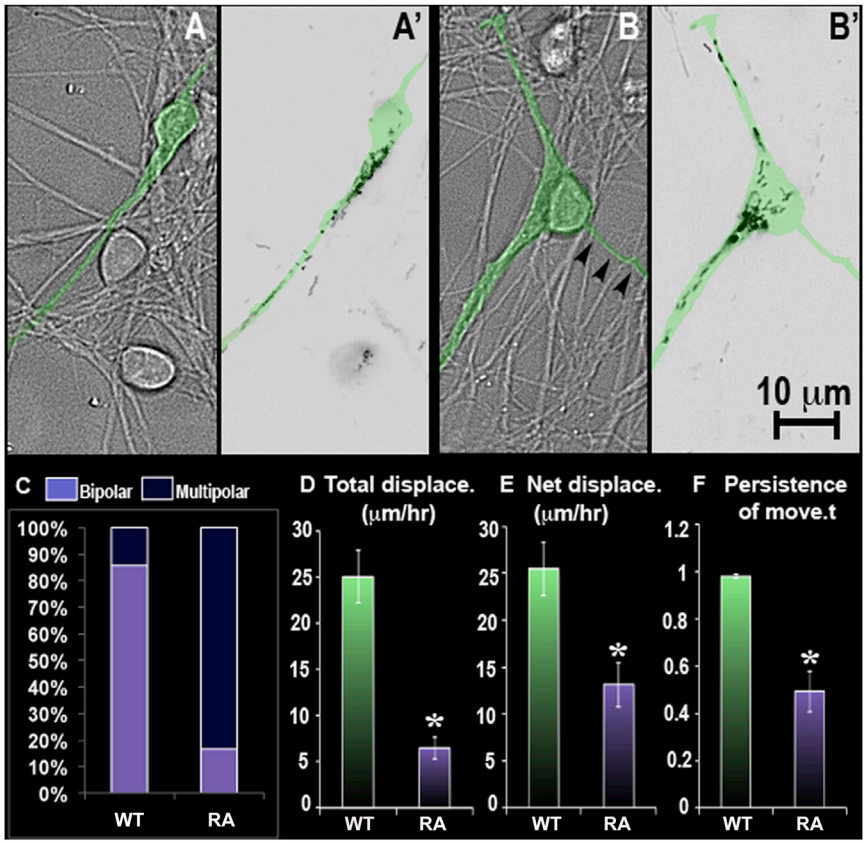


Figure 4. Expression of dsRed-Tagged Wild-Type or Mutant Dominant-Negative MgcRacGAP in Cultured Cerebellar Granule Neurons

(A and A′) Differential interference contrast (DIC) and inverted epifluorescence still images, respectively, of neurons transfected with wild-type MgcRacGAP construct.

(B and B′) DIC and inverted epifluorescence still images, respectively, of neurons transfected with mutant (RA) MgcRacGAP construct. Arrowheads in (B) indicate the thinner of the three processes, with MgcRacGAP entering the other two. The transfected neuron is digitally colored green in the top four panels.

(C) Analyses of morphology of migrating neurons transfected with the wild-type versus mutant (RA) construct.

(D and E) Quantification of average total displacement and average net displacement per hour for wild-type and mutant groups.

(F) Quantification of persistence of movement for wild-type and mutant groups.

See also Figure S4.

respectively). In kinesin-6-depleted cells, the proportion of comets directed away from the centrosome in the soma region was similar to controls (95.3% ± 1.7%, p = 0.7), but there was a significant decrease in comets directed away from the centrosome in the leading process (70.2% ± 1.5%, p = 0.02, n = 9 cells in each group; Figure S3C). Notably, no significant difference was observed in the orientation of comets directed away from the centrosome in the process that was not the leader at that point of time, in comparison with the leading process in controls (92.5% ± 2.5%, p = 0.8, Student's t test, n = 9 cells in each group). Thus, unlike the actin enrichment, which could appear simultaneously in two processes, the microtubule defect resulting from kinesin-6 depletion was specific to the process serving as the leader at any moment in time. We suspect that this reflects a role for kinesin-6 in maintaining microtubule organization in the face of major alterations in the actin cytoskeleton and/or in directing which process will take possession of the actin enrichment, thus becoming the leader.

### MgcRacGAP in Migratory Neurons

A Rho-family GTPase-activating protein called MgcRacGAP combines during cytokinesis with kinesin-6 to form a complex called centralspindlin that binds to microtubules in the spindle midzone and regulates F-actin localization via a downstream signaling cascade [9–13]. If this same situation obtains in migratory neurons, the two proteins should track together. Conducting time-lapse imaging on neurons transfected with a dsRed-tagged MgcRacGAP construct, we found the tagged protein to localize in the leading process and soma in a distribution that colocalized with kinesin-6 in immunostain analyses. As the neurons migrated, we observed the tagged MgcRacGAP moving through these cellular compartments, with cotransfected EGFP marking the outline of the cell. For multiple cells (n = 14 cells, n = 27 instances of forward stepping of soma), quantitative analyses of the tagged MgcRacGAP revealed it moving to concentrate in the proximal region of the process serving as the leader, in a fashion similar to the F-actin enrichment (see Figure S4 for details). In kinesin-6-depleted neurons that displayed normal bipolar morphology, MgcRacGAP distribution resembled that of controls, whereas kinesin-6-depleted multipolar cells showed MgcRacGAP in more than one process simultaneously (Figure S4C).

A GAP-inactive version of the construct called MgcRacGAP-RA is known to act as a dominant negative [22]. Comparison of control neurons (i.e., not kinesin-6 depleted) transfected with wild-type MgcRacGAP or MgcRacGAP-RA indicated that whereas the wild-type protein was localized in the leading process, the mutant protein was distributed in two different processes (Figures 4A, 4A′, 4B, and 4B′). Time-lapse imaging indicated that while neurons transfected with wild-type MgcRacGAP exhibited net displacement of 25 ± 2.9 μm/hr (n = 14 cells) and total displacement of 25.5 ± 2.8 μm/hr, the MgcRacGAP-RA group exhibited net displacement and total displacement of 6.5 ±1.2 μm/hr (n = 12 cells) and 13.2 ±2.4 μm/hr, respectively. Persistence of movement was also different for these two groups (Figures 4D–4F). A significantly higher proportion of cells transfected with MgcRacGAP-RA exhibited multipolar morphology (83.3%) compared to those transfected with wild-type MgcRacGAP (14.3%; Figure 4C). These effects on migration closely resembled those resulting from kinesin-6 depletion, consistent with a cytokinesis-like pathway functioning in migrating neurons. This view is buoyed by previous findings that RhoA (the target of MgcRacGAP signaling) also accumulates in the leading process [23].

We previously reported that kinesin-6 helps establish the mixed orientation of dendritic microtubules [24, 25], presumably via a sliding microtubule mechanism consistent with the properties of kinesin-6 to transport minus ends of

microtubules toward plus ends of other microtubules [26]. Our present findings, consistent with the strong expression of kinesin-6 in migratory neurons [27], indicate that kinesin-6 plays another, earlier role in neuronal development. In migratory neurons, kinesin-6 is not essential to concentrate F-actin in the proximal region of processes, but it is essential to constrain the F-actin concentration to a single process. Such constraint appears to be critical for enabling the neuron to designate a single process as the leader and hence to enable the centrosome to follow that process in an orderly fashion. The role of kinesin-6 in neuronal migration borrows a mechanistic theme from cytokinesis, one of the most fundamental cytoskeletal pathways in nature, with the proximal region of the leading process being analogous to the cleavage furrow.

#### Supplemental Information

Supplemental Information includes four figures, Supplemental Experimental Procedures, and one movie and can be found with this article online at http://dx.doi.org/10.1016/j.cub.2013.05.027.

#### Acknowledgments

All surgeries followed Tata Institute Animal Ethics Committee guidelines and were performed in the Tata Institute animal breeding facility. This work was funded by grants from the National Institutes of Health (R01NS28785) and the National Science Foundation (0841245) to P.W.B., as well as from the Department of Biotechnology, Government of India to S.T. and from the Priority Academic Program Development of Jiangsu Higher Education Institutions and National Natural Science Foundation grant 31171007 to M.L. We thank K. Kadam of the Tata Institute for performing the in utero electroporations and I. Fischer, X. Yuan, K. Toyo-oka, and W. Yu (Drexel University) for helpful discussions. A.F. is the recipient of the Doris Willig, MD Award from the Drexel University College of Medicine Institute for Women's Health and Leadership. S.T. is the recipient of the Shanti Swarup Bhatnagar Prize for Science and Technology.

Received: January 11, 2013
Revised: April 2, 2013
Accepted: May 14, 2013
Published: June 20, 2013

#### References

1. Edmondson, J.C., and Hatten, M.E. (1987). Glial-guided granule neuron migration in vitro: a high-resolution time-lapse video microscopic study. J. Neurosci. *7*, 1928–1934.
2. Solecki, D.J., Model, L., Gaetz, J., Kapoor, T.M., and Hatten, M.E. (2004). Par6alpha signaling controls glial-guided neuronal migration. Nat. Neurosci. *7*, 1195–1203.
3. Solecki, D.J., Trivedi, N., Govek, E.E., Kerekes, R.A., Gleason, S.S., and Hatten, M.E. (2009). Myosin II motors and F-actin dynamics drive the coordinated movement of the centrosome and soma during CNS glial-guided neuronal migration. Neuron *63*, 63–80.
4. Tsai, J.W., Bremner, K.H., and Vallee, R.B. (2007). Dual subcellular roles for LIS1 and dynein in radial neuronal migration in live brain tissue. Nat. Neurosci. *10*, 970–979.
5. Bellion, A., Baudoin, J.P., Alvarez, C., Bornens, M., and Metin, C. (2005). Nucleokinesis in tangentially migrating neurons comprises two alternating phases: forward migration of the Golgi/centrosome associated with centrosome splitting and myosin contraction at the rear. J. Neurosci. *25*, 5691–5699.
6. Ma, X., Kawamoto, S., Hara, Y., and Adelstein, R.S. (2004). A point mutation in the motor domain of nonmuscle myosin II-B impairs migration of distinct groups of neurons. Mol. Biol. Cell *15*, 2568–2579.
7. Schaar, B.T., and McConnell, S.K. (2005). Cytoskeletal coordination during neuronal migration. Proc. Natl. Acad. Sci. USA *102*, 13652–13657.
8. Glotzer, M. (2009). The 3Ms of central spindle assembly: microtubules, motors and MAPs. Nat. Rev. Mol. Cell Biol. *10*, 9–20.
9. Mishima, M., Kaitna, S., and Glotzer, M. (2002). Central spindle assembly and cytokinesis require a kinesin-like protein/RhoGAP complex with microtubule bundling activity. Dev. Cell *2*, 41–54.
10. Pavicic-Kaltenbrunner, V., Mishima, M., and Glotzer, M. (2007). Cooperative assembly of CYK-4/MgcRacGAP and ZEN-4/MKLP1 to form the centralspindlin complex. Mol. Biol. Cell *18*, 4992–5003.
11. Barr, F.A., and Gruneberg, U. (2007). Cytokinesis: placing and making the final cut. Cell *131*, 847–860.
12. Bement, W.M., Benink, H.A., and von Dassow, G. (2005). A microtubule-dependent zone of active RhoA during cleavage plane specification. J. Cell Biol. *170*, 91–101.
13. Somers, W.G., and Saint, R. (2003). A RhoGEF and Rho family GTPase-activating protein complex links the contractile ring to cortical microtubules at the onset of cytokinesis. Dev. Cell *4*, 29–39.
14. Sarkisian, M.R., Frenkel, M., Li, W., Oborski, J.A., and LoTurco, J.J. (2001). Altered interneuron development in the cerebral cortex of the flathead mutant. Cereb. Cortex *11*, 734–743.
15. Di Cunto, F., Imarisio, S., Hirsch, E., Broccoli, V., Bulfone, A., Migheli, A., Atzori, C., Turco, E., Triolo, R., Dotto, G.P., et al. (2000). Defective neurogenesis in citron kinase knockout mice by altered cytokinesis and massive apoptosis. Neuron *28*, 115–127.
16. Tsai, J.W., Chen, Y., Kriegstein, A.R., and Vallee, R.B. (2005). LIS1 RNA interference blocks neural stem cell division, morphogenesis, and motility at multiple stages. J. Cell Biol. *170*, 935–945.
17. Falnikar, A., Tole, S., and Baas, P.W. (2011). Kinesin-5, a mitotic microtubule-associated motor protein, modulates neuronal migration. Mol. Biol. Cell *22*, 1561–1574.
18. Noctor, S.C., Martínez-Cerdeño, V., Ivic, L., and Kriegstein, A.R. (2004). Cortical neurons arise in symmetric and asymmetric division zones and migrate through specific phases. Nat. Neurosci. *7*, 136–144.
19. Tabata, H., and Nakajima, K. (2003). Multipolar migration: the third mode of radial neuronal migration in the developing cerebral cortex. J. Neurosci. *23*, 9996–10001.
20. Nichols, A.J., Carney, L.H., and Olson, E.C. (2008). Comparison of slow and fast neocortical neuron migration using a new in vitro model. BMC Neurosci. *9*, 50.
21. Kuriyama, R., Gustus, C., Terada, Y., Uetake, Y., and Matuliene, J. (2002). CHO1, a mammalian kinesin-like protein, interacts with F-actin and is involved in the terminal phase of cytokinesis. J. Cell Biol. *156*, 783–790.
22. Hirose, K., Kawashima, T., Iwamoto, I., Nosaka, T., and Kitamura, T. (2001). MgcRacGAP is involved in cytokinesis through associating with mitotic spindle and midbody. J. Biol. Chem. *276*, 5821–5828.
23. Guan, C.B., Xu, H.T., Jin, M., Yuan, X.B., and Poo, M.M. (2007). Long-range Ca2+ signaling from growth cone to soma mediates reversal of neuronal migration induced by slit-2. Cell *129*, 385–395.
24. Lin, S., Liu, M., Mozgova, O.I., Yu, W., and Baas, P.W. (2012). Mitotic motors coregulate microtubule patterns in axons and dendrites. J. Neurosci. *32*, 14033–14049.
25. Sharp, D.J., Yu, W., Ferhat, L., Kuriyama, R., Rueger, D.C., and Baas, P.W. (1997). Identification of a microtubule-associated motor protein essential for dendritic differentiation. J. Cell Biol. *138*, 833–843.
26. Nislow, C., Lombillo, V.A., Kuriyama, R., and McIntosh, J.R. (1992). A plus-end-directed motor enzyme that moves antiparallel microtubules in vitro localizes to the interzone of mitotic spindles. Nature *359*, 543–547.
27. Ferhat, L., Kuriyama, R., Lyons, G.E., Micales, B., and Baas, P.W. (1998). Expression of the mitotic motor protein CHO1/MKLP1 in postmitotic neurons. Eur. J. Neurosci. *10*, 1383–1393.